www.nature.com/aps

Acta Pharmacologica Sinica

ARTICLE

Dectin-1 plays a deleterious role in high fat diet-induced NAFLD of mice through enhancing macrophage activation

Min-xiu Wang[1], Wu Luo[1,2], Lin Ye[1], Lei-ming Jin[1], Bin Yang[1], Qian-hui Zhang[1], Jian-chang Qian[1], Yi Wang[1], Yi Zhang[3] and Guang Liang[1,3]

The innate immune response and inflammation contribute to hepatic steatosis and non-alcoholic fatty liver disease (NAFLD). Dectin-1 is a pathogen recognition receptor in innate immunity. In this study, we investigated the role of Dectin-1 in the pathogenesis of NAFLD. We first showed that Dectin-1 expression was significantly elevated in liver tissues of patients with NASH. NAFLD was induced in mice by feeding high fat diet (HFD) for 24 weeks. At the end of treatment, mice were sacrificed, and their blood and liver tissues were collected for analyses. We showed HFD feeding also increased liver Dectin-1 levels in mice, associated with macrophage infiltration. Either gene knockout or co-administration of a Dectin-1 antagonist laminarin (150 mg/kg twice a day, ip, from 16th week to 24th week) largely protected the livers from HFD-induced lipid accumulation, fibrosis, and elaboration of inflammatory responses. In primary mouse peritoneal macrophages (MPMs), challenge with palmitate (PA, 200 μM), an abundant saturated fatty acid found in NAFLD, significantly activated Dectin-1 signaling pathway, followed by transcriptionally regulated production of pro-inflammatory cytokines. Dectin-1 was required for hepatic macrophage activation and inflammatory factor induction. Condition media generated from Dectin-1 deficient macrophages failed to cause hepatocyte lipid accumulation and hepatic stellate activation. In conclusion, this study provides the primary evidence supporting a deleterious role for Dectin-1 in NAFLD through enhancing macrophage pro-inflammatory responses and suggests that it can be targeted to prevent inflammatory NAFLD.

Keywords: non-alcoholic fatty liver disease; Dectin-1; macrophages; NF-κB; TGF-β1; inflammation

Acta Pharmacologica Sinica (2023) 44:120–132; https://doi.org/10.1038/s41401-022-00926-2

INTRODUCTION

Non-alcoholic fatty liver disease (NAFLD) is a spectrum of liver disease that includes steatosis, fibro-inflammatory reactions, and hepatocellular degeneration [1], that ultimately progresses to cirrhosis. The more severe form of NAFLD, non-alcoholic steatohepatitis (NASH) is less common and affects ~6.5 % of the general population [2]. The high prevalence of NAFLD is in part due to its strong association with metabolic syndrome, including obesity, insulin resistance and diabetes, and dyslipidemia [3, 4]. To date, no treatments targeting NASH have shown conclusive benefits.

Pathogenesis of NAFLD is complex and has traditionally been described related to two important features seen in the disease: lipid accumulation and chronic inflammation. Hepatocytes uptake the excess fatty acids [5] and this, together with increased de novo lipogenesis [6], leads to hepatic lipid accumulation. Toxicity of the accumulated lipids and the activation of the innate immune system then drive NAFLD. Immune mechanisms involving macrophages and other cells such as dendritic cells recognizing damage- and pathogen-associated molecular patterns contribute to the progression of the inflammatory cascade. As one of the most studied cell types in innate immunity, macrophages have drawn particular attention because macrophage proinflammatory activation is highly associated with hepatic steatosis and inflammation [7]. The combined effect of these fundamental cellular processes ultimately lead to the activation of hepatic stellate cells, increases in collagen deposition, and hepatic fibrogenesis [8]. Accordingly, therapeutic strategy targeting these innate immunity receptors, signaling molecules, and inflammatory mediators may attenuate NAFLD.

Dectin-1, a pathogen recognition receptor (PRR) in innate immunity, belongs to the C-type lectin receptor family and it is expressed mainly on myeloid cells. Dectin-1 is a small type-II transmembrane protein containing a carbohydrate recognition domain and is specifically expressed in macrophages and other myeloid-monocytic lineage cells [9]. Dectin-1 can recognize β-glucans in fungal pathogens and then mediate pro-inflammatory intracellular signals, including spleen tyrosine kinase (Syk) [10, 11] and nuclear factor-κB (NF-κB) [12, 13]. After binding of β-glucans, such as zymosan, Dectin-1 can induce cytokines and chemokines, including TNF-α [14, 15], CXC-chemokine ligand 2 [16], and interleukins (ILs) [15]. Soon after its discovery, studies started to emerge that showed broad activity of Dectin-1, well beyond those against fungal and non-fungal pathogens. For example, increased

[1]Chemical Biology Research Center, School of Pharmaceutical Sciences, Wenzhou Medical University, Wenzhou 325035, China; [2]Medical Research Center, the First Affiliated Hospital, Wenzhou Medical University, Wenzhou 325035, China and [3]School of Pharmaceutical Sciences, Hangzhou Medical College, Hangzhou 311399, China
Correspondence: Guang Liang (wzmcliangguang@163.com)
These authors contributed equally: Min-xiu Wang, Wu Luo.

Received: 2 March 2022 Accepted: 24 May 2022
Published online: 10 June 2022

levels of Dectin-1 have been found in inflammatory bowel disease lesions [17]. Dectin-1 was shown to be important for the natural killer cell-dependent tumor toxicity due to the high levels of N-glycan structures in the tumors [18]. Yan's group found that Dectin-1 also contributes to myocardial ischemia/reperfusion injury by regulating macrophage polarization and infiltration [19]. Therefore, Dectin-1 may represent a therapeutic target in the treatment of non-infectious inflammatory diseases, possibly including NAFLD. A study of thioacetamide- and carbon tetrachloride-induced acute liver injury, however, showed a protective role of Dectin-1 in hepatic fibrosis [20]. Whether Dectin-1 contributes to NAFLD and the potential underlying mechanisms are largely unknown.

Given these, there is a critical need to elucidate the exact role for Dectin-1 in the development and progression of NAFLD. The present study shows that Dectin-1 is increased in human NASH, and in the mouse model of high-fat diet (HFD)-induced NAFLD. We provide the primary evidence to support a deleterious role for Dectin-1 in NAFLD, and this role of Dectin-1 is likely mediated through enhancing macrophage pro-inflammatory response. Either gene knockout or pharmacological inhibition of Dectin-1 attenuated NAFLD in mice. Therefore, our studies have identified a novel role of Dectin-1 in the pathogenesis of NAFLD.

MATERIALS AND METHODS

Antibodies and general reagents

Antibodies against macrophage marker F4/80 (cat# sc-377009), SMAD2/3 (cat# sc-133098), CD68 (cat# sc-9139) were purchased from Santa Cruz Biotechnology (Dallas, TX, USA). Antibodies against Dectin-1 (cat# ab140039) and smooth muscle actin-alpha (α-SMA, cat# ab5694) were purchased from Abcam (Cambridge, UK). Antibodies for p-Syk at Tyr352 (cat# 2717), Syk (cat# 13198), IκBα (cat# 4812), phospho-NF-κB p65 (cat# 3033), and NF-κB p65 (cat# 8242) were purchased from Cell Signaling Technology (Danvers, MA, USA). Antibodies against Collagen Type I (Col-1, cat# 14695-1-AP), HA tag (cat# 66006-2-Ig), DYKDDDDK tag (Binds to FLAG® tag epitope, cat# 20543-1-AP), TNF-α (cat# 60291-1-Ig), and TGF-β1 (cat# 21898-1-AP) were purchased from Proteintech (Rosemont, IL, USA). GAPDH antibody (cat# AB-P-R001) was from Hangzhou Goodhere Biotechnology (Hangzhou, China). DyLight 488-conjugated Goat Anti-Mouse IgG (cat# A23210) and DyLight 549-conjugated Goat Anti-Rabbit IgG (cat# A23420) antibodies were purchased from Abbkine (Wuhan, China). Horseradish peroxidase-conjugated Goat Anti-Mouse IgG (cat# A0216) and Horseradish peroxidase-conjugated Goat Anti-Rabbit IgG (cat# A0208) antibodies were from Beyotime Biotechnology (Shanghai, China).

Pierce ECL Western Blotting Substrate and diaminobenzidine (DAB) were purchased from Thermo Fisher (Waltham, MA, USA). Laminarin [21] (LAM; cat# hrl-lam) was purchased from Invivogen (San Diego, CA, USA). Assay kits for total cholesterol (TCH; cat# A111-1-1), triglyceride (TG; cat# A110-1-1), low-density lipoprotein-cholesterol (LDL-C; cat# A113-1-1), alkaline phosphatase (AKP; cat# A059-2-2), total bilirubin (T-BIL; cat# C019-1-1), alanine aminotransferase (ALT; cat# C009-2-1), and aspartate aminotransferase (AST; cat# C010-2-1) were purchased from Nanjing Jiancheng Bioengineering Institute (Nanjing, China). TGF-β1 ELISA kit (cat# 70-EK981-96) was obtained from Multi Sciences (Hangzhou, China). Mouse TNF-α and IL-6 cytokine ELISA kits (cat# 88-7324-76 and cat# 88-7064-76) were from Invitrogen (Waltham, MA, USA). Masson's Trichrome Stain Kit (cat# 1340), Hematoxylin and Eosin (H&E) staining kit (cat# G1120), Sirius red (cat# S8060), and Oil-Red O staining solution (cat# G1261) were purchased from Solarbio Life Sciences (Beijing, China). Sodium palmitate (PA; cat# P9767-5G) and bovine serum albumin (BSA; cat# A1933) were purchased from Sigma (Louis, MO, USA). A working solution of 5 mM PA was prepared by heating PA to 80 °C and adding it to 5% BSA maintained at 55 °C.

Cell culture

Primary mouse peritoneal macrophages (MPMs) were prepared from C57BL/6 wildtype and Dectin-1$^{-/-}$ mice, essentially as described previously [22]. To validate Dectin-1 disruption functionally in MPMs derived from Dectin-1$^{-/-}$ mice, cells were exposed to 200 μM palmitate for 24 h and culture medium was used to measure transforming growth factor-β1 (TGF-β1) levels. For some studies, conditioned media generated following exposure of MPMs to PA were applied to primary hepatocytes and human hepatic stellate cell line LX-2 cells. LX-2 cells (cat# CL-0560) [23] were purchased from Procell Life Science & Technology (Wuhan, China) and cultured in high-glucose containing DMEM (cat# C11960500BT, Gibco, Eggenstein, Germany) with 10% fetal bovine serum (FBS, cat# 10099141C, Gibco, Eggenstein, Germany), 1% penicillin/streptomycin (cat# 1514-0122, Invitrogen, Carlsbad, CA, USA).

HEK-293T cell line (cat# SCSP-502) was purchased from Shanghai Institute of Biochemistry and Cell Biology (Shanghai, China) and cultured in high-glucose containing DMEM with 10% FBS, 1% penicillin/streptomycin. HEK-293T cells were used to express Flag- and HA-tagged Dectin-1. Briefly, pcDNA3.1 expressing Dectin-1-Flag and -HA plasmids were applied to HEK-293T cells using LipofectAMINE™ 2000 (cat# 11688-019, Invitrogen, Carlsbad, CA, USA).

Primary mouse hepatocytes were isolated from C57BL/6J wildtype and Dectin-1$^{-/-}$ mice by a modified two-step collagenase perfusion procedure. After anesthesia, liver tissues were perfused with medium comprising of 0.5 mM EGTA and 10 mM glucose in 1× HBSS using a pump rate of 6–7 mL/min input through the hepatic portal vein and output postcava. A collagenase digestion solution medium was prepared and consisted of 1 mM $CaCl_2$, 10 mM glucose, and 0.4 mg/mL collagenase type-2 (cat# LS004176, Worthington, Lakewood, CO, USA) in 1× HBSS. Digestion medium was preheated and applied for 15 min, with postcava clipping every 1 min. After digestion, liver tissues were manually disrupted with forceps in Williams E Medium (cat# W4125, Sigma, Louis, MO, USA). The supernatant, containing hepatocytes, was passed through a 100-μm filter into 50-mL tubes. To remove parenchymal cells, 10 mL of the single-cell suspension was added to 10 mL Percoll solution (cat# p4937, Sigma, Louis, MO, USA). Tubes were spun at 200 × *g* for 10 min at 4 °C. The cell pellet was then resuspended in Williams E Medium containing 10% FBS, 100 U/mL penicillin, and 100 mg/mL streptomycin, and plated in cell culture dishes. Nonadherent cells were removed 4–6 h after seeding.

Primary mouse Kupffer cells (KCs) were isolated from C57BL/6J wildtype and Dectin-1$^{-/-}$ mice by a modified two-step collagenase perfusion procedure. The digestion steps are the same as primary mouse hepatocytes isolation. After digestion, liver tissues were manually disrupted with forceps in RMPI-1640 Medium (cat# C11875500BT, Gibco, Eggenstein, Germany). After centrifugation for 3 min at 50 × *g*, 4 °C, the supernatant containing the non-parenchymal cells was collected and this step was repeated two times, for a total of three washes. After centrifugation at 500 × *g* for 3 min, 4 °C, the supernatant was removed. The cell pellet was then resuspended in RMPI-1640 medium containing 10% FBS, 100 U/mL penicillin, and 100 mg/mL streptomycin, and plated in cell culture dishes. Nonadherent cells were removed 2 h after seeding.

Animal experiments

Mouse studies were initiated following review and approval of care and experimental procedures by Wenzhou Medical University Animal Policy and Welfare Committee (Approval Document No. wydw2020-0117). All animal experiments conformed the NIH

guidelines (Guide for the care and use of laboratory animals). Twelve male Dectin-1$^{-/-}$ mice on a C57BL/6 background and 30 male C57BL/6 mice weighing 18–22 g were obtained from GemPharmatech (Nanjing, China). The Dectin-1 knockout allele has the sequences corresponding to the cytoplasmic tail, transmembrane, and stalk regions of the Dectin-1 locus (*Clec7a*) deleted [24]. Mice were housed in a pathogen-free room under 22 ± 2 °C, 50%–60% humidity, 12:12 h light-dark cycle.

Twelve male C57BL/6 wildtype (WT) mice were randomly divided into two groups: low-fat diet (WT-LFD) and high-fat diet (WT-HFD). Similarly, 12 male Dectin-1$^{-/-}$ mice were divided into Dectin-1$^{-/-}$-LFD and Dectin-1$^{-/-}$-HFD. Each group had 6 mice. LFD group was fed with a standard rodent diet (cat #MD12031, MediScience Diets Co., Ltd., Yangzhou, China). HFD consisted of 60 kcal.% fat, 20 kcal.% protein, and 20 kcal.% carbohydrates (cat. #MD12033). Mice were fed these diets for 24 weeks. At the end of treatment, mice were sacrificed under sodium pentobarbital (i.p. injection of 0.2 mL sodium pentobarbital at 100 mg/mL) for anesthesia and pain medication. Blood and liver tissues were collected at the conclusion of the study. Liver function in mice was assessed by measuring serum ALT and AST levels. Total serum levels of TG, TCH, T-BIL, AKP, and LDL-C were measured using commercially available kits.

We also administered Dectin-1 inhibitor LAM [21] to mice. Eighteen male C57BL/6 mice were randomly divided into three groups: LFD, HFD, and HFD + LAM ($n = 6$). Mice in LFD and HFD were fed the respective diets as indicated above. For the HFD + LAM group, LAM was administered at 150 mg/kg twice a day by intraperitoneal injection (in PBS) from 16th week to 24th week. Mice were sacrificed and the blood and liver samples were obtained at 24th week, as indicated above.

Liver tissues were sectioned and performed to H&E, Sirius Red, and Masson's Trichrome staining, respectively. NAFLD activity score (NAS) was calculated by using the NASH-clinical research network (CRN) criteria [25]. Liver tissues were also immunohistochemically examined with Dectin-1, CD68, or TNF-α antibodies. Lipid accumulation in liver tissues was detected by Oil Red O staining. Circulating cytokines were determined in serum samples using TNF-α and IL-6 ELISA kits.

Human liver samples

All procedures involving human samples followed the principles in the Declaration of Helsinki and were approved by the Review Ethics Committee in Human of the First Affiliated Hospital of Wenzhou Medical University (Approval No. 2019-032). Human liver samples were obtained from the First Affiliated Hospital of Wenzhou Medical University. Hepatic steatosis specimens ($n = 6$) were collected from patients with NASH who had undergone liver biopsy, and non-steatotic liver tissues ($n = 6$) were obtained from individuals diagnosed with liver hemangioma and hepatic cyst and accepted liver surgeries. The histological features and clinical information of NASH patients are listed in Supplementary Table S1.

Liver tissue staining

Liver tissues were fixed in 4% paraformaldehyde, embedded in paraffin, and sectioned at 5-μm thickness. After dehydration, sections were stained with H&E. Stained sections were evaluated for general histopathological damage using light microscopy. Additional paraffin sections were stained with Sirius Red and Masson's Trichrome Stain to assess liver fibrosis. NAS was calculated by using the NASH-CRN criteria [26].

For immunohistochemistry, sections were deparaffinized, hydrated, and subjected to heat-induced antigen retrieval (0.01 M sodium citrate buffer, pH = 6.0). Slides were blocked with 3% hydrogen peroxide for 30 min and in 1% BSA for 30 min and incubated with Dectin-1, CD68, or TNF-α antibodies (1:100) overnight at 4 °C. Horseradish peroxidase-labeled secondary antibodies were then applied for 1 h at 37 °C. Immunoreactivity was detected by DAB. Slides were counterstained with hematoxylin. Images were acquired using a Nikon microscope (Nikon, Japan). ImageJ analysis software version 1.53i (NIH; Bethesda, MD, USA) was used to determine staining-positive cells.

Immunofluorescence staining of liver tissues was performed using frozen tissues in Optimal Cutting Temperature (OCT) media. Tissues were sectioned at 5-μm thickness. Sections were fixed in formalin for 10 min, blocked with 1% BSA for 1 h, and then incubated with primary antibodies at 4 °C overnight. Fluorophore-conjugated secondary antibodies were applied for 1 h at room temperature. Sections were counterstained with DAPI and imaged using an epi-fluorescence microscope (Nikon, Japan).

Lipid staining in cells and tissues

Lipid accumulation in liver tissues was detected by Oil Red O staining. Frozen liver tissues in OCT media were sectioned at 7 μm-thick sections. Sections were fixed in 10% formalin for 10 min, followed by 100% propylene glycol for 10 min at room temperature. Sections were then incubated with Oil-Red O solution for 10 min. A 60% propylene glycol solution was added for 1 min. Nuclei were stained in hematoxylin. To detect lipid accumulation in culture studies, cells were fixed in 10% formalin for 10 min and then placed in 100% propylene glycol for 10 min at room temperature. After fixation, cells were stained with Oil Red O working solution for 10 min. Images were acquired.

Cytokine measurements

For in vitro studies, secreted cytokines were determined from a conditioned medium. Cells from these studies were collected for total protein concentration determination. The level of TGF-β1 in the MPMs conditioned media was determined using a commercial ELISA kit. For mouse studies, circulating cytokines were determined in serum samples using TNF-α and IL-6 ELISA kits. OD_{450} was measured with SpectraMax M5 microplate reader (Molecular Devices; Silicon Valley, CA, USA). The level of cytokines was normalized to total protein measurements (BCA Protein Assay, cat# 23225; Thermo Fisher).

Western blot and immunoprecipitation

Cell and tissue lysates were prepared in RIPA buffer (cat# P0013B; Beyotime Biological Technology, Shanghai, China) and protein concentration was measured. Protein lysates were separated by sodium dodecyl sulfate-polyacrylamide gel electrophoresis and transferred to polyvinylidene fluoride membranes. Membranes were blocked in Tris-buffered saline (pH 7.4, containing 0.05% Tween 20 and 5% non-fat milk) for 1 h at room temperature and incubated with primary antibodies at 4 °C overnight. Secondary antibodies were applied for 1 h at room temperature. Immunoreactivity was visualized using enhanced chemiluminescence reagent (Bio-Rad) and quantified using ImageJ analysis software version 1.53i. Values were normalized to respective housekeeping proteins.

Protein-protein binding was evaluated by co-immunoprecipitation combined with immunoblotting. Cellular total protein was extracted using cell lysis buffer for IP (cat# P0013; Beyotime) containing protease inhibitor cocktail. Protein lysates (100–500 μg) were incubated with precipitating antibody at 4 °C overnight, then immunoprecipitated with protein A/G agarose beads and shaking at room temperature for 2 h. The bead-protein complexes were collected by centrifugation, then washed three times with PBS. Finally, the complex was dissociated by heating and target protein was blotted through Western blot and corresponding immunoblotting antibody.

Real-time qPCR

mRNA levels were detected by real-time qPCR. Total RNA was extracted from cells and tissues using TRIzol Reagent (Thermo

Fisher, Waltham, MA, USA). RNA was reverse-transcribed using PrimeScript RT reagent (cat# RR047A, Takara Bioscience, Japan). Real-time PCR was subsequently conducted using TB Green Premix Ex Taq II (cat# RR820A, Takara, Japan) on CFX96 Touch Real-Time PCR Detection System (Bio-Rad, Hercules, CA, USA). Relative expression was calculated by $2^{-\Delta\Delta Ct}$ method with *Actb* normalization. Primer sequences are listed in Supplementary Table S2.

MTT assay

Different time periods of exposure to condition medium were selected to examine stellate cell growth through the MTT assay. Briefly, LX-2 cells were plated in 96-well plates and cultured overnight at 37 °C. The next day, cells were exposed to condition media from MPMs. At different times, cell viability was measured by adding MTT reagent (cat# M8180-250MG, Solarbio, Beijing, China) to each well for 4 h. The reaction was stopped by adding *N*, *N*-dimethylformamide and the absorbance was read at 490 nm. Optical density measures were reported. To supplement this assay, gene and protein markers of stellate activation were performed.

Statistical analysis

All experiments are randomized and blinded. All data are reported as mean ± SEM. Statistical analysis was performed with GraphPad Prism 8.0 software (San Diego, CA, USA). We used one-way ANOVA followed by Dunnett's post hoc test when comparing more than two groups of data and one-way ANOVA, nonparametric Kruskal–Wallis test, followed by Dunnett's post hoc test when comparing multiple independent groups. *P* values less than 0.05 were considered to be statistically significant. Post-tests were run only if *F* achieved $P < 0.05$ and there was no significant variance inhomogeneity.

RESULTS

Dectin-1 is elevated in liver tissues of subjects with NASH and high-diet fed mice

The involvement of Dectin-1 in NAFLD/NASH has not been reported. Here, we studied the expression of Dectin-1 in human liver samples from subjects with NASH and compared the results to levels found in subjects with other indications such as hemangiomas and hepatic cysts. Our results indicate that Dectin-1 is elevated in subjects with diagnosed NASH (Fig. 1a, c). We next examined Dectin-1 levels in an experimental model of NAFLD. To do this, we utilized the HFD model to produce hepatic steatosis and NASH-like features in mice [27]. In this model, 24-week duration of HFD increased Dectin-1 levels in liver tissues compared to mice fed a LFD (Fig. 1b, d, e). We next stained the mouse liver tissues to examine which cell types express Dectin-1. Previous studies have reported that Dectin-1 is mainly expressed in macrophages or myeloid cells [18, 20]. Double immunofluorescence staining of mouse tissues revealed that Dectin-1 immunoreactivity to be co-localized with F4/80 macrophage marker (Fig. 1f). It is also indicated that increased Dectin-1 level in liver tissues may come from the increased hepatic macrophage infiltration in NAFLD mice. These data establish increased Dectin-1 in human and experimental NAFLD and confirm macrophage as the likely cell type expressing Dectin-1.

Dectin-1 mediates HFD-induced liver injury and lipid accumulation

To understand the role of Dectin-1 in NAFLD, we fed wildtype and Dectin-1 knockout mice a HFD for 24 weeks (Fig. 2a) and examined their livers (Fig. 2b). Since Dectin-1 is well-known myeloid cell-specific protein, we establish Dectin-$1^{-/-}$ mice using whole-body knockout techniques (Supplementary Fig. S1). In this model, HFD increased body weights compared to LFD in both wildtype and Dectin-$1^{-/-}$ mice (Supplementary Fig. S2). No effect of Dectin-1 deficiency alone was noted. Wildtype mice fed a HFD had increased liver weight to tibia length ratio indicating enlarged livers (Fig. 2c). However, this enlargement was not seen in Dectin-$1^{-/-}$ mice fed a HFD. Serum alanine transaminase (ALT) and aspartate transaminase (AST) enzyme levels were also increased in wildtype mice fed a HFD but not in Dectin-$1^{-/-}$ mice when compared to their respective LFD controls (Fig. 2d, e). Similar results were obtained when alkaline phosphatase (AKP) and total bilirubin (T-BIL) were measured (Fig. 2f, g).

Histological examination of liver tissues showed obvious signs of excessive lipid accumulation in wildtype mice on HFD (Fig. 2h). Although lipid accumulation can also be seen in Dectin-$1^{-/-}$ mice fed an HFD, the levels are appreciably lower compared to wildtype mice. We then utilized the NAS [28] to assess liver injury. Our results show significantly higher NAS for wildtype mice on HFD compared to LFD (Fig. 2i), validating the experimental model. Liver tissues of Dectin-$1^{-/-}$ mice, however, showed no significant changes induced by HFD (Fig. 2i). We also measured lipid accumulation by staining liver tissues with Oil Red O, a neutral lipid dye, which further showed that Dectin-1 deficiency prevented the excessive lipid accumulation in HFD mice (Fig. 2j, k). Serum lipid profile also showed increased LDL-cholesterol, triglycerides, and total cholesterol in wildtype mice but not in Dectin-$1^{-/-}$ mice on HFD (Fig. 2l-n). Confirming these results, mRNA levels of fat metabolizing enzymes (*Srebp1c, Acac1, Cpt1a*) in liver tissues were observed to be increased in wildtype mice on HFD (Fig. 2o). As expected, Dectin-1 deficient mice did not show these gene inductions. These results show that Dectin-1 deficiency prevents against HFD-induced hepatic lipid accumulation and liver dysfunction.

Dectin-1 mediates HFD-induced liver fibrosis and inflammatory responses

As mentioned, previous study has shown that Dectin-1 is involved in hepatic fibrosis [20]. Specifically, researchers showed that Dectin-1 deficiency increased thioacetamide- and carbon tetrachloride-induced liver fibrosis. To examine whether Dectin-1 is involved in liver fibrosis in the HFD model of NAFLD, we stained liver tissues of mice with Picro Sirus Red and Masson's Trichrome. However, both assays showed that HFD induced fibrosis only in wildtype mice and Dectin-1 knockout significantly reduced HFD-induced hepatic fibrosis (Fig. 3a-d). Protein and mRNA levels of fibrosis-associated factors (Col1, α-SMA, and TGF-β) confirmed this protective role of Dectin-1 deficiency in NAFLD (Fig. 3e–h).

Next, we stained the liver tissues of wildtype and Dectin-$1^{-/-}$ mice for macrophage marker CD68 and TNF-α to assess inflammatory responses to HFD. Increased CD68 and TNF-α immunoreactivity was noted in wildtype mouse liver tissues upon HFD feeding (Fig. 4a–d). Serum TNF-α and IL-6 levels were also increased in wildtype mice fed a HFD (Fig. 4e, f). As expected, CD68 and TNF-α staining in liver tissues, and serum TNF-α and IL6 levels showed marked reductions in Dectin-$1^{-/-}$-HFD mice when compared to wildtype mice on HFD (Fig. 4a–f). We then measured mRNA levels of various inflammatory factors including cytokines and adhesion molecules. These studies confirmed increased inflammatory responses in wildtype mice upon HFD but not in Dectin-$1^{-/-}$ mice (Fig. 4g–i). To measure signaling proteins, downstream of Dectin-1, in liver tissues, we probed for Syk [29, 30] and NF-κB [31]. Although Dectin-1 signaling pathway is just emerging, studies have shown that Dectin-1 activation recruits and then phosphorylates Syk to activate pro-inflammatory transcriptional factor NF-κB. Based on these studies, we probed liver tissue lysates for phosphorylated (p-) Syk and p65 subunit of NF-κB. We also measured the levels of inhibitor of κB as a measure of NF-κB activity. Our results show that increased p-Syk and p-p65, and reduced IκBα levels in lysates prepared from wildtype mice fed a HFD compared to mice fed an LFD (Fig. 4J, Supplementary Fig. S3). Dectin-$1^{-/-}$ mice did not show these changes of Syk and NF-κB activations in liver.

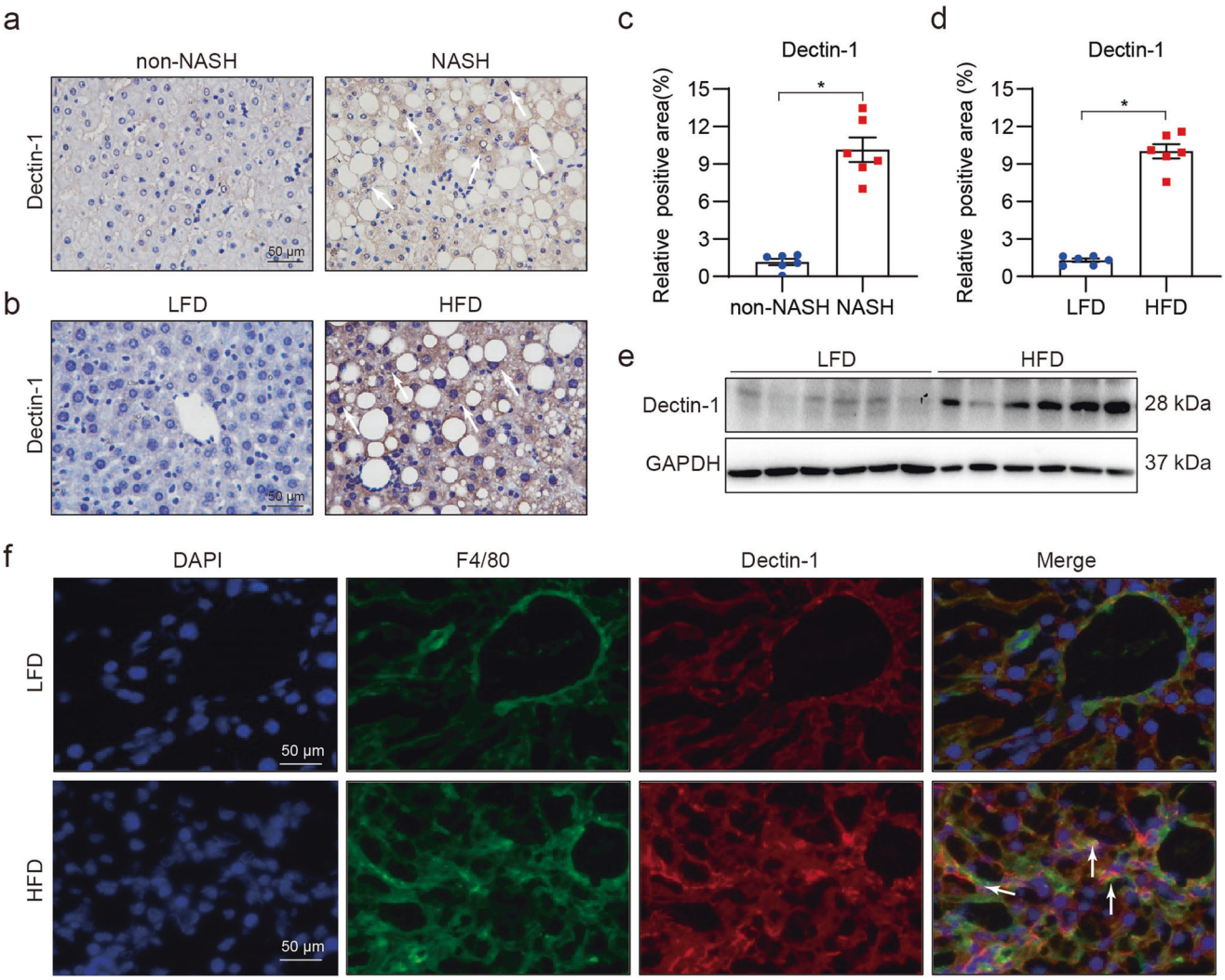

Fig. 1 Dectin-1 is increased in liver tissues of patients with NASH and in mice fed a high-fat diet. a, **c** Dectin-1 immunoreactivity in liver tissues of patients with NASH. Liver tissues from subjects with other indications were used as normal. Immunoreactivity was detected by DAB (brown). Sections were counterstained with hematoxylin (blue). Quantification of immunoreactive area is shown in **c** (scale bar = 50 μm; $n = 6$; Mean ± SEM; $^*P < 0.05$). **b**, **d** Liver tissues of C57Bl/6 mice fed a low-fat diet (LFD) or a high-fat diet (HFD) for 24 weeks were examined for Dectin-1 immunoreactivity. Staining quantification is shown in **d** (scale bar = 50 μm; $n = 6$; Mean ± SEM; $^*P < 0.05$). **e** Representative Western blot analysis of Dectin-1 in liver tissue from LFD- and HFD-fed mice. GAPDH was used as loading control ($n = 6$). **f** Representative immunofluorescence staining of liver tissues of mice. Figure showing macrophage marker F4/80 (green) and Dectin-1 (red) in liver samples from mice fed LFD and HFD. Tissues were counterstained with DAPI (blue) (scale bar = 50 μm; $n = 6$).

Laminarin administration in mice mimic Dectin-1 deficiency and protects against HFD-induced liver injury

To strengthen our findings, we repeated the HFD experimental platform in wildtype mice but treated the mice with LAM. LAM is a (1→3, 1→6)-β glucan and is reported to be a Dectin-1 antagonist [21]. LAM binds to Dectin-1 and inhibits its association with particulate β(1–3)-glucans [32, 33]. To reach a therapeutic effect, we initiated HFD feeding in mice, and on 16th week started to administer LAM (Supplementary Fig. S4a). Mice were then followed up at 24th week (Supplementary Fig. S4b). Analysis of liver ALT and AST showed that LAM reduced HFD-induced increases (Supplementary Fig. S4c, d), indicating preservation of liver function. Histological analysis also showed that LAM reduced signs of lipid accumulation and NAS injury values in the HFD-fed mice (Supplementary Fig. S5a–d). Similarly, LAM administration was associated with reduced levels of liver fibrosis upon HFD as evident through Sirius Red and Masson's Trichrome staining of liver tissues (Supplementary Fig. S5e–h), and immunoblotting for fibrosis-associated factors in tissues lysates (Supplementary Fig. S5i, j). Assessment of inflammatory cytokine mRNA in liver tissues revealed the protective effect of LAM on HFD-induced increases (Supplementary Fig. S6a, b). This is not surprising as Dectin-1$^{-/-}$ mice showed the same blunted inflammatory response to HFD feeding. Mechanisms mediating these protective effects also appeared to be similar since LAM showed reduced p-Syk and p-p65, and increased IκBα levels in liver lysates of HFD-fed mice (Supplementary Fig. S6c, d). Together, these results confirmed that pharmacological LAM treatment of mice mimics Dectin-1 deficiency and preserves liver function in mice challenged with long-term HFD feeding.

Palmitate (PA)-induced inflammatory responses in macrophages are mediated by Dectin-1

To understand how Dectin-1 may mediate liver injury in response to HFD, we used an in vitro system of challenging primary macrophages with palmitate (PA), since Dectin-1 is mainly expressed in myeloid cells [34]. This experimental setup is based on the premise that NAFLD is characterized as an inflammatory

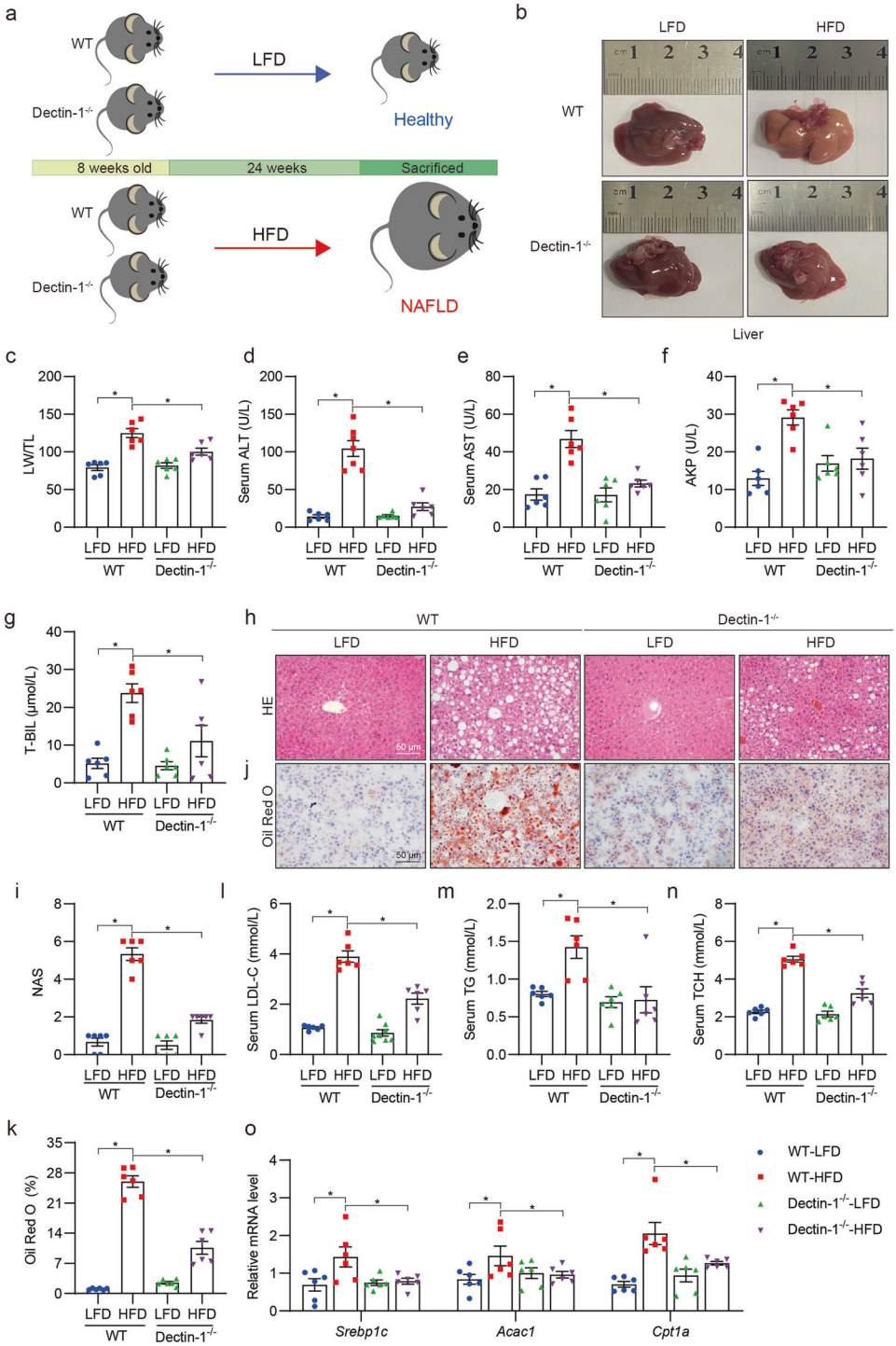

Fig. 2 Dectin-1 knockout mice are protected against HFD-induced lipid accumulation in the liver. a The schematic diagram shows the grouping and steps of animal experiments. WT and Dectin-1$^{-/-}$ mice were fed with low-fat rodent diet (LFD) or high-fat diet (HFD) for 24 weeks. **b** Gross images of liver tissues harvested from wildtype (WT) and Dectin-1 knockout (Dectin-1$^{-/-}$) mice after 24 weeks on LFD and HFD. **c** Measurements of liver weight/tibia length (LW/TL) in mice ($n = 6$; Mean ± SEM; *$P < 0.05$). **d**–**g** Serum levels of ALT (**d**), AST (**e**), ALT/AKP (**f**), and T-BIL (**g**) in mice ($n = 6$; Mean ± SEM; *$P < 0.05$). **h** Representative H&E-stained liver sections (scale bar = 50 μm). **i** NAFLD activity score was determined based on histopathological changes in the liver tissues of mice ($n = 6$; Mean ± SEM; *$P < 0.05$). **j**, **k** Assessment of lipid accumulation in liver tissues using Oil Red O staining. Representative staining images are shown in **i** (scale bar = 50 μm). Quantification of staining is shown in **j** ($n = 6$; Mean ± SEM; *$P < 0.05$). Levels of serum LDL-C (**l**), TG (**m**), and TCH (**n**) in mice ($n = 6$; Mean ± SEM; *, $P < 0.05$). **o** mRNA levels of fatty acid metabolism genes (*Srebp1c, Acac1, Cpt1a*) in liver tissues of mice fed a LFD and HFD. Transcripts were normalized to *Actb* ($n = 6$; Mean ± SEM; *$P < 0.05$).

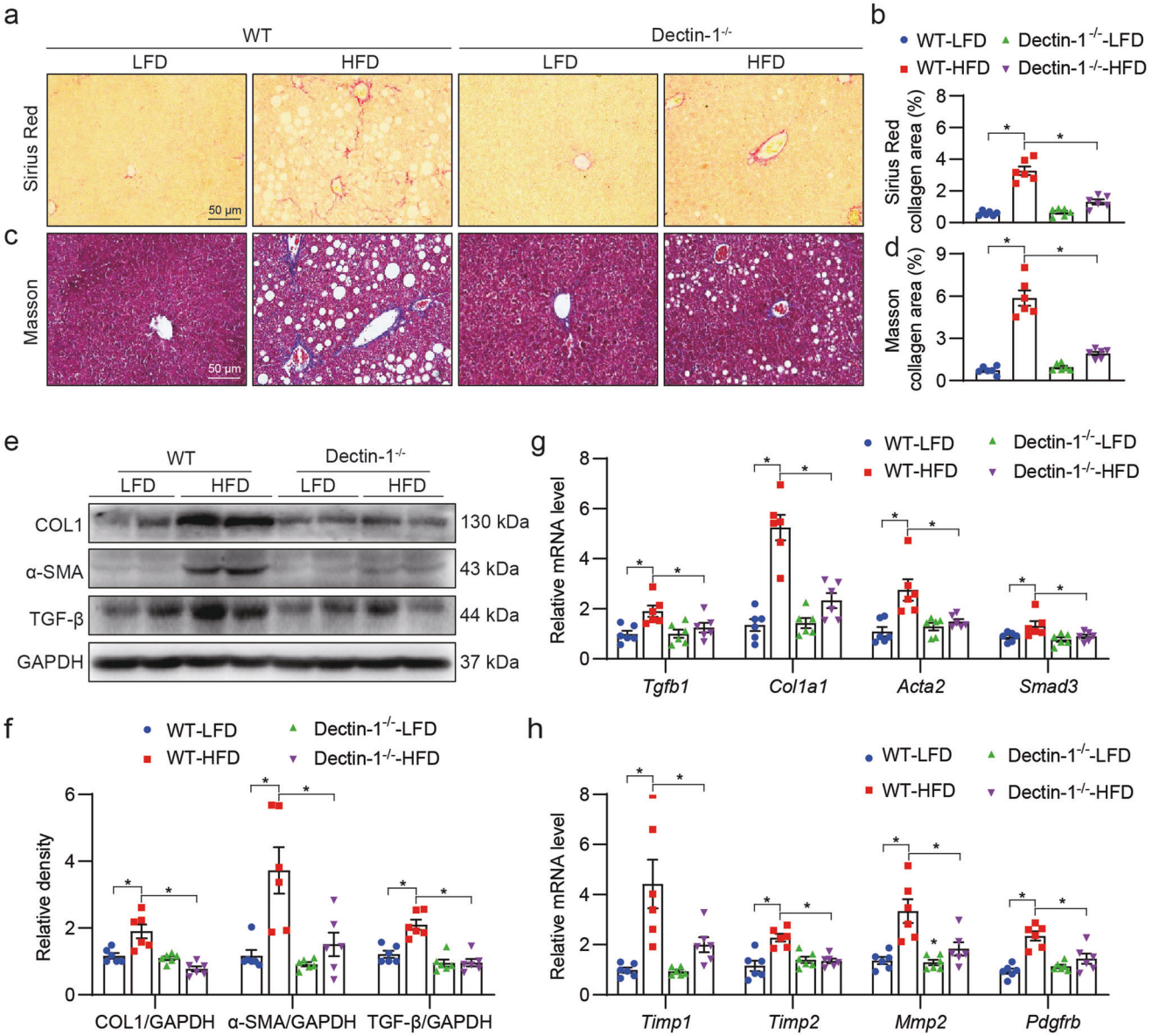

Fig. 3 **Dectin-1 deficiency prevents HFD-induced liver fibrosis in mice. a**, **b** Excessive collagen deposition in liver tissues of mice fed a HFD was measured by Picro Sirius Red (red) staining. Representative stained images are shown in (**a**) and quantification of staining area in (**b**) ($n = 6$; Mean ± SEM; *$P < 0.05$). **c**, **d** Masson's Trichrome staining was used to determine fibrosis in liver tissues (blue). Representative stained images are shown in **c** and quantification of staining area in (**d**) ($n = 6$; Mean ± SEM; *$P < 0.05$). Measurement of fibrosis-related proteins in liver tissue lysates. Representative immunoblots (**e**) and densitometric quantification (**f**) are shown. GAPDH was used as control. Representative stained images are shown in (**a**) and quantification of staining area in (**b**) ($n = 6$; Mean ± SEM; *$P < 0.05$). mRNA levels of fibro-genic genes (**g**) and matrix remodeling genes (**h**) were measured. Transcripts were normalized to *Actb* ($n = 6$; Mean ± SEM; *$P < 0.05$).

process induced by elevated concentration of free fatty acids, including palmitate [34, 35]. To carry out detailed investigations on the mechanisms, we first transfected HEK-293T cells with flag- and HA-tagged Dectin-1 (Fig. 5a, b). Exposure of transfected HEK-293T cells to 200 μM PA caused increased association between Flag- and HA-tagged Dectin-1 (Fig. 5c, Supplementary Fig. S7a), indicating Dectin-1 dimerization by PA stimulation. However, when cells were pretreated with LAM at 200 μg/mL, this increased interaction was not seen. We then harvested primary mouse peritoneal macrophages (MPMs) from C57BL/6 mice and exposed the cells to PA. Increased Dectin-1-Syk interaction was observed by co-immunoprecipitation (Fig. 5d, Supplementary Fig. S7b). Again, LAM pretreatment of MPMs prevented this interaction. To confirm these results, we isolated MPMs from Dectin-$1^{-/-}$ mice and showed that subsequent in vitro exposure to PA fails to increase p-Syk and p-p65, or reduce IκBα levels as seen in MPMs from wildtype mice (Fig. 5e, Supplementary Fig. S7c). Pretreatment of wildtype MPMs with LAM generated the same result as seen in Dectin-$1^{-/-}$ MPMs (Fig. 5f, Supplementary Fig. S7d). We further stained the cells for p65 to examine subcellular localization and noted increased nuclear levels in response to PA in MPMs isolated from wildtype mice (Fig. 5g, Supplementary Fig. S7e). Nuclear translocation of NF-κB was significantly reduced in Dectin-$1^{-/-}$ MPMs exposed to PA, and the results were consistent with immunoblotting studies. Similar results were observed when PA-challenged MPMs were treated with LAM (Supplementary Fig. S7f, g). Downstream of NF-κB, inflammatory factors expression was seen in setting of intact Dectin-1(Fig. 5h, Supplementary Fig. S7h–j). As we know, liver-inhabited macrophages (Kupffer cells, KCs) also contribute to the hepatic

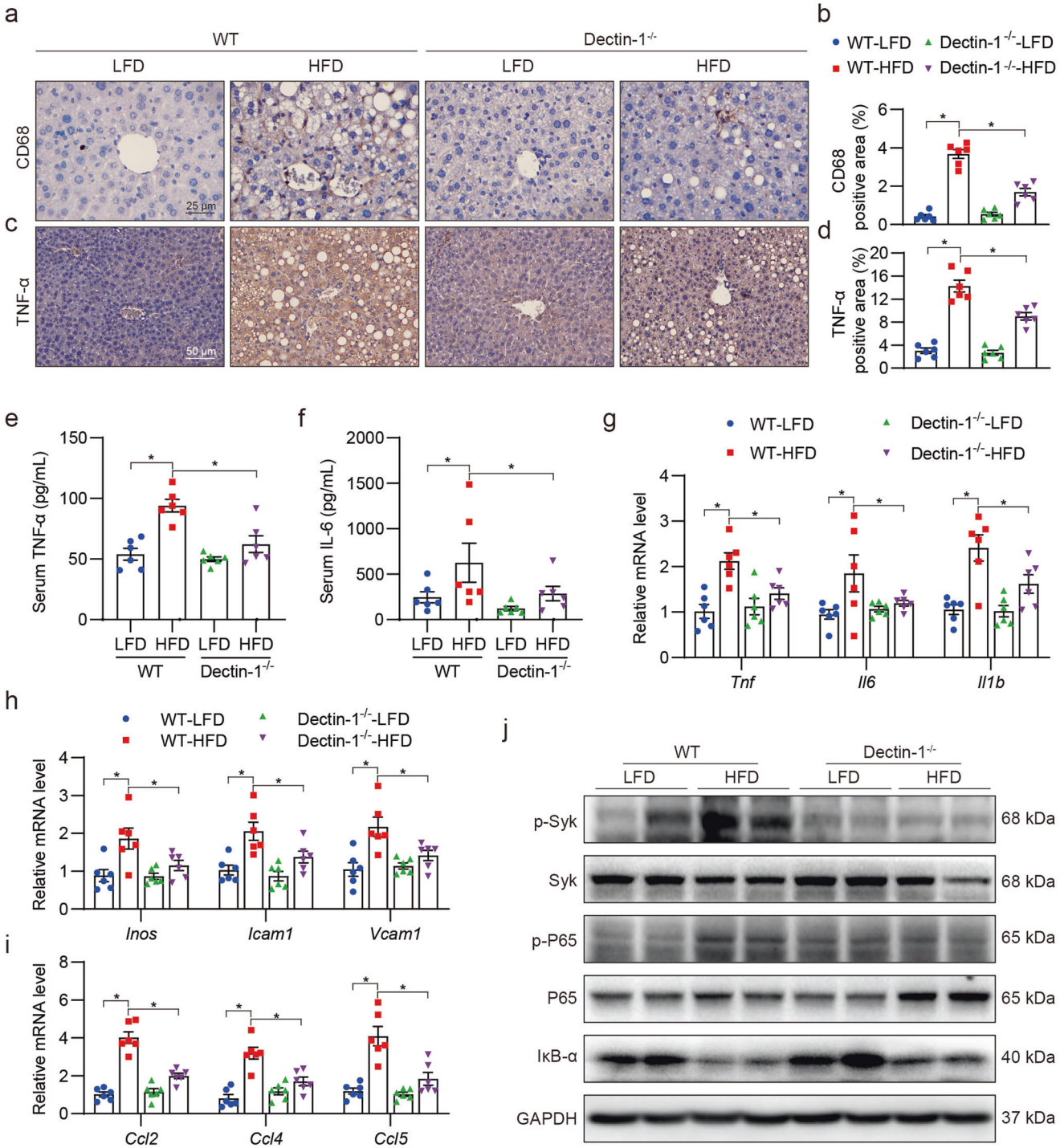

Fig. 4 Reduced inflammatory responses are exhibited in liver tissues of Dectin-1 knockout mice fed an HFD. a, **b** Staining of liver tissues of mice fed a LFD and a HFD for macrophage marker CD68. Sections were counterstained with hematoxylin (blue). Representative staining images of CD68 (brown) are shown in (**a**) and quantification in (**b**) ($n = 6$; Mean ± SEM; *$P < 0.05$). **c**, **d** Levels of TNF-α in liver tissues as detected by immunohistochemistry. Representative stained images are shown in **c** (brown) and quantification of staining is shown in (**d**) ($n = 6$; Mean ± SEM; *$P < 0.05$). **e**, **f** Serum levels of TNF-α and IL-6 in mice ($n = 6$; Mean ± SEM; *$P < 0.05$). **g**–**i** mRNA of inflammatory response genes in liver tissues of mice fed a LFD and a HFD. Transcripts were normalized to *Actb* ($n = 6$; Mean ± SEM; *, $P < 0.05$). **j** Immunoblot analysis of NF-κB p65, Syk, and IκBα in liver tissues. Phosphorylated proteins and total proteins were measured (Mean ± SEM; $n = 6$; *$P < 0.05$).

inflammation and steatosis in NAFLD. To explore the role of Dectin-1 in KCs, primary mouse KCs were isolated from wildtype and Dectin-$1^{-/-}$ mice and then exposed to 200 μM PA. The mRNA levels of inflammatory factors (*Tnf*, *Il6*, *Ccl2*, and *Icam1*) were significantly reduced in Dectin-$1^{-/-}$ KCs exposed to PA (Fig. 5i). We also measured the protein levels of IL-6 and TNF-α secreted by wildtype and Dectin-$1^{-/-}$ KCs exposed to PA and found that these proteins were increased only in wildtype KCs (Fig. 5j, k). These results show that PA induces Dectin-1 and downstream Syk-NF-κB pathway activation and then inflammatory factors expression in both infiltrating and inhabited macrophages.

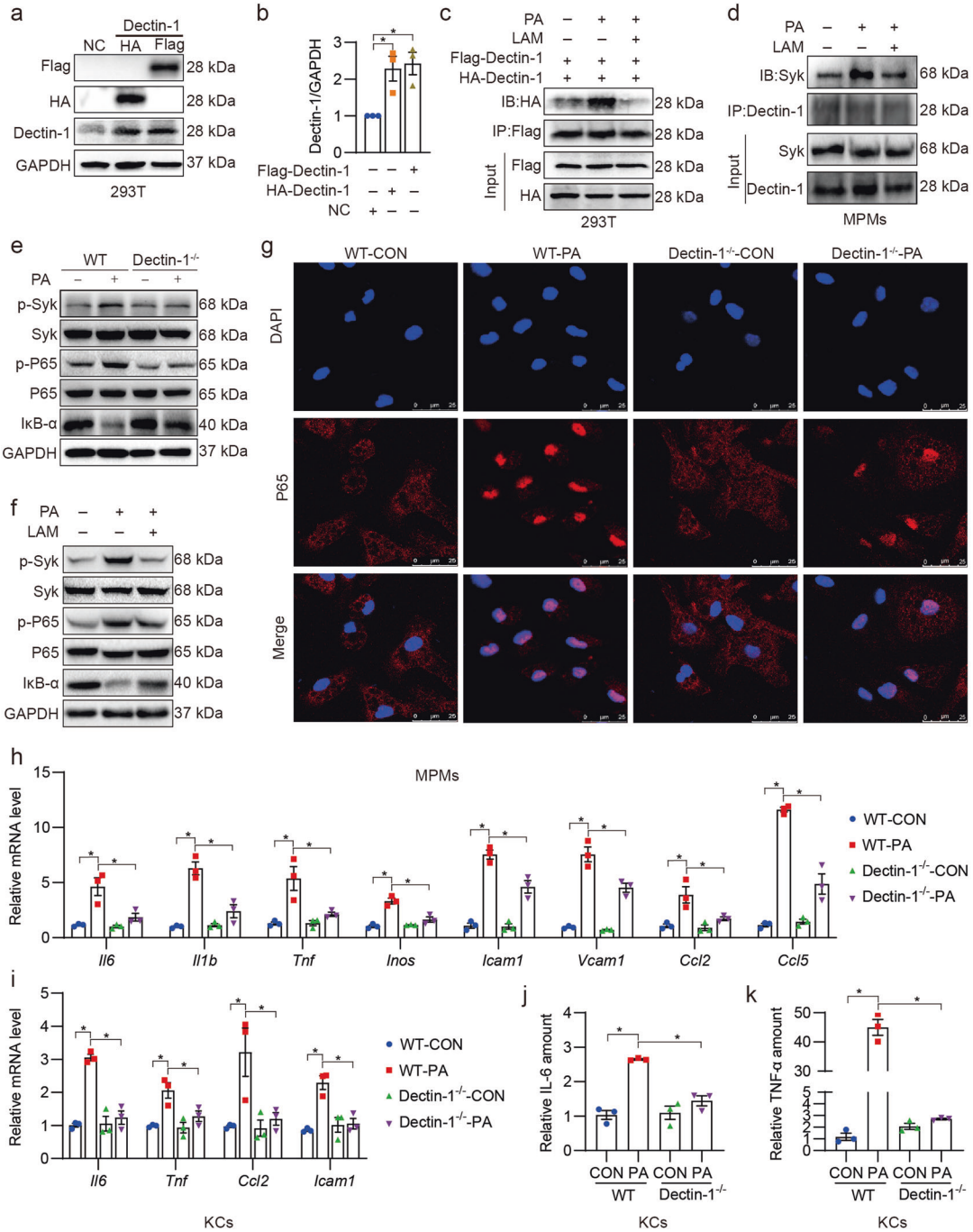

Fig. 5 **PA mediates pro-inflammatory Syk/NF-κB activation in macrophages through Dectin-1. a**, **b** HEK-293T cells were transfected with Flag- and HA-tagged Dectin-1 plasmids. Control cells were transfected with empty vector (negative control; NC). Levels of Flag-tag, HA-tag, and Dectin-1 proteins were measured by immunoblotting. GAPDH was used as a loading control. Densitometric quantification is shown in **b** (Mean ± SEM; $n = 3$; $^*P < 0.05$). **c** Following transfection with Flag- and HA-tagged Dectin-1 plasmids, HEK-293T cells were pretreated with 200 μg/mL laminarin (LAM) for 1 h and then exposed to 200 μM PA for 1 h. Dectin-1 dimerization was measured by immunoprecipitation. **d** MPMs harvested from wildtype mice were pretreated with 200 μg/mL LAM for 1 h and then exposed to 200 μM PA for 1 h. The interaction between Dectin-1 (IP) and Syk (IB) was assessed by co-immunoprecipitation. **e** MPMs harvested from wildtype (WT) and Dectin-$1^{-/-}$ mice were exposed to 200 μM PA or vehicle for 1 h. Immunoblot analysis of p-Syk/Syk, IκBα, and p-p65/p65 was performed. GAPDH was used as a loading control. **f** MPMs from wildtype mice were pretreated with or without 200 μg/mL LAM for 1 h and then exposed to 200 μM PA for 1 h. Immunoblot analysis of p-Syk/Syk, IκBα, and p-p65/p65 was performed. GAPDH was used as a loading control. **g** MPMs harvested from wildtype (WT) and Dectin-$1^{-/-}$ mice were exposed to 200 μM PA or vehicle for 1 h. Cells were stained p65 subunit of NF-κB (red). Cells were counterstained with DAPI (blue). **h** mRNA levels of inflammatory factors were measured in WT and Dectin-$1^{-/-}$ MPMs exposed to 200 μM PA for 12 h. Transcripts were normalized to *Actb* ($n = 3$; Mean ± SEM; $^*P < 0.05$). **i** mRNA levels of inflammatory factors were measured in WT and Dectin-$1^{-/-}$ KCs exposed to 200 μM PA for 12 h. Transcripts were normalized to *Actb* ($n = 3$; Mean ± SEM; $^*P < 0.05$). **j**, **k** KCs harvested from wildtype (WT) and Dectin-$1^{-/-}$ mice were exposed to 200 μM PA for 24 h. Levels of IL-6 and TNF-α in condition media were measured ($n = 3$; Mean ± SEM; $^*P < 0.05$).

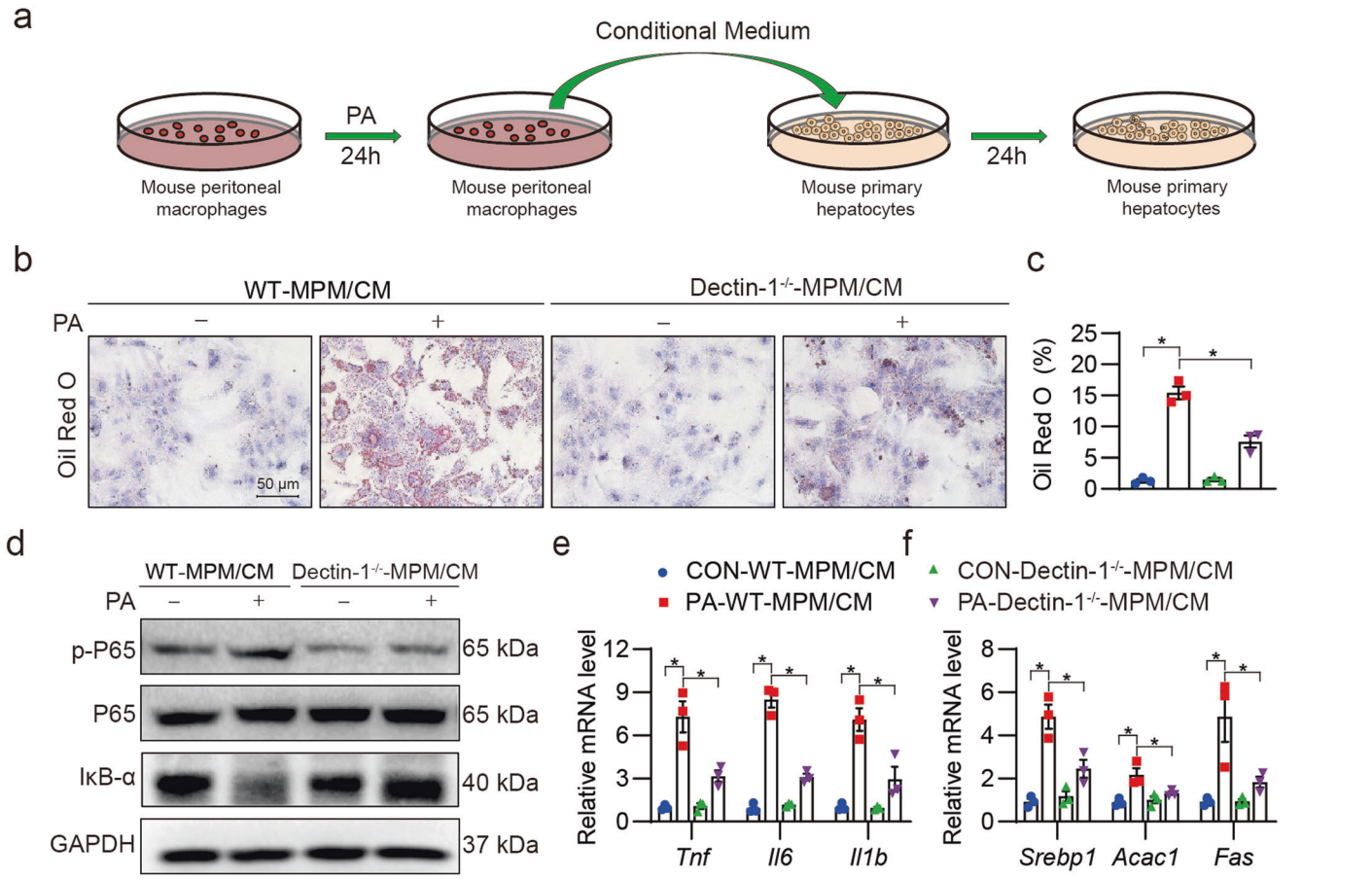

Fig. 6 Dectin-1-deficient macrophage factors fail to induce hepatocyte lipid accumulation and inflammatory responses. a Schematic showing experimental design. MPMs, derived from WT and Dectin-1$^{-/-}$ mice, were exposed to 200 μM PA or vehicle control for 24 h. Condition media (CM) was collected and applied to primary hepatocytes at 1:1 ratio with fresh media. Hepatocytes were examined after 24 h. **b**, **c** Lipid accumulation in hepatocytes in response to MPM-CM from WT or Dectin-1$^{-/-}$ mice exposed vehicle (CON) or PA was determined by Oil Red O staining. Representative stained cells are shown in (**b**) and quantification of lipid accumulation is shown in (**c**) (scale bar = 50 μm; $n = 3$; Mean ± SEM; *$P < 0.05$). **d** Immunoblot analysis of IκBα and p-p65/p65 in hepatocytes. Cells were exposed to MPM/CM as indicated in (**b**) and (**c**). GAPDH was used as loading control. mRNA levels of inflammatory factors (**e**) and genes involved in fibrosis and fatty acid metabolism (**f**). Hepatocytes were treated as indicated in (**b**) and (**c**). Transcripts were normalized to *Actb* ($n = 3$; Mean ± SEM; *$P < 0.05$).

Dectin-1-driven macrophage inflammatory factors enhance hepatocyte fat deposition and inflammatory responses

Previous studies have already shown that inflammatory cytokines released by macrophages could induce lipid metabolism dysfunction and inflammation in hepatocytes [36]. Next, we examined how macrophage-derived inflammatory factors (e.g.,: *Tnf, Il6*, and *Il1b*) may alter hepatocytes to generate NAFLD-like phenotype. To do this, we cultured MPMs from wildtype and Dectin-1$^{-/-}$ mice and exposed the cells to 200 μM PA. We then collected the condition media (CM) and applied it to primary mouse hepatocytes (Fig. 6a). Even a short exposure of hepatocytes to CM from wildtype MPM challenged with PA, increased Oil Red O staining indicating lipid accumulation (Fig. 6b, c). However, when CM from Dectin-1$^{-/-}$ MPMs, challenged identically as wildtype MPMs, was applied to hepatocytes, no significant increases in Oil Red O staining were seen. We probed hepatocyte lysates in this experiment for NF-κB activation and show increased p-p65 levels and reduced IκBα levels when wildtype MPM CM was applied (Fig. 6d, Supplementary Fig. S8a). Application of Dectin-1$^{-/-}$ MPM CM did not lead to NF-κB activation. Induction of inflammatory factors and lipid metabolism genes (*Srebp1*, *Acac1*, and *Fas*) was also not seen in hepatocytes exposed to Dectin-1$^{-/-}$ MPM CM, compared to CM from wildtype MPMs (Fig. 6e, f). These results indicate that intact Dectin-1 in macrophages is needed to generate factors leading to hepatocyte lipid metabolic dysfunction and accumulation.

Dectin-1-driven TGF-β1 in macrophages promote activation hepatic stellate cells

Hepatic stellate cells are considered to play an important role in hepatic fibrogenesis [37, 38]. In this setting, TGF-β1 is one of the key drivers of stellate activation [39, 40]. We measured the levels of TGF-β1 in CM of wildtype and Dectin-1$^{-/-}$ MPMs exposed to PA and showed increases in wildtype MPMs only (Fig. 7a). Similar results were observed in CM of wildtype and Dectin-1$^{-/-}$ KCs exposed to PA (Fig. 7b). No such PA-induced increases were seen in MPMs harvested from Dectin-1$^{-/-}$ mice. We then examined whether macrophage-derived factors, including TGF-β1, activate hepatic stellate cells by applying CM to human LX-2 stellate cell line (Fig. 7c). Wildtype MPM CM generated following PA exposure increased LX-2 cell number of a 96-h period, indicating cell growth (Fig. 7d). However, CM from Dectin-1$^{-/-}$ MPMs did not generate the same response. mRNA and protein markers of stellate activation and fibrosis increased following exposure of LX-2 cells to wildtype MPM CM but not CM prepared from Dectin-1$^{-/-}$ MPMs (Fig. 7e–h, Supplementary Fig. S8b). These results show that macrophage Dectin-1 is needed for the induction of hepatic stellate activation in response to PA/HFD.

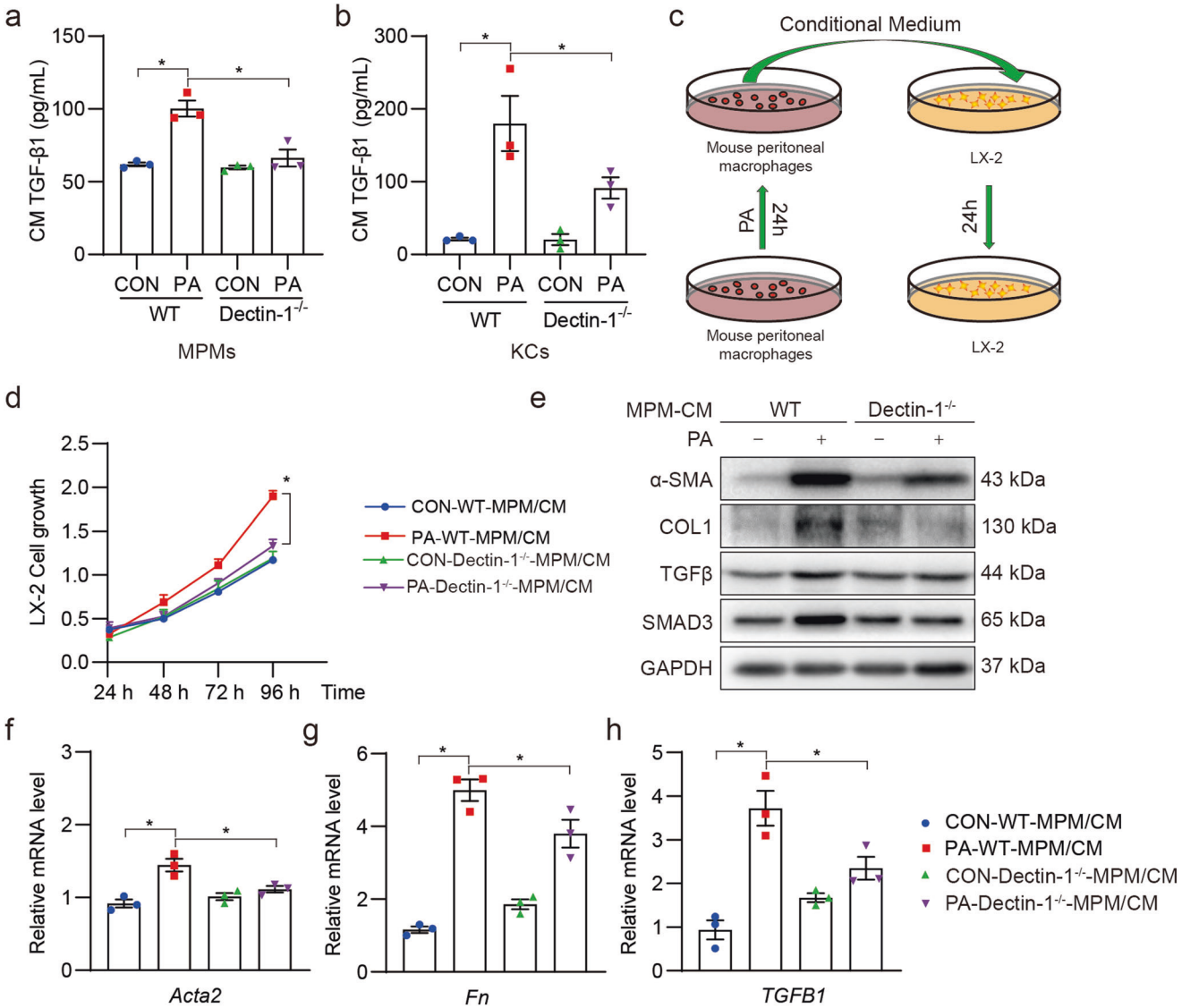

Fig. 7 Dectin-1 is required in macrophages to activate hepatic stellate cells. a MPMs harvested from wildtype (WT) and Dectin-1$^{-/-}$ mice were exposed to 200 μM PA or vehicle control (CON) for 24 h. Levels of TGF-β1 in condition media were measured ($n = 3$; Mean ± SEM; *$P <$ 0.05). **b** KCs harvested from wildtype (WT) and Dectin-1$^{-/-}$ mice were exposed to 200 μM PA or vehicle control (CON) for 24 h. Levels of TGF-β1 in condition media were measured ($n = 3$; Mean ± SEM; *$P < 0.05$). **c** Schematic showing experimental setup of hepatic stellate cell activation. Condition media from MPMs exposed to PA or vehicle control were prepared and applied to LX-2 stellate cells. **d** Effect of MPM condition media (MPM/CM) on LX-2 growth determined by *OD* value over 96 h. MPMs were prepared from wildtype (WT) and Dectin-1$^{-/-}$ mice and exposed to 200 μM PA or vehicle control (CON) for 24 h ($n = 3$; Mean ± SEM; *$P < 0.05$). **e** Immunoblot analysis of fibrosis-related proteins in LX-2 cells exposed to CM from MPMs for 24 h. GAPDH was used as loading control. **f**–**h** mRNA levels of stellate activation genes were measured in LX-2 cells exposed to MPM/CM. Transcripts were normalized to *Actb* ($n = 3$; Mean ± SEM; *$P < 0.05$).

DISCUSSION

In the present study, we have examined the potential role of the innate immune receptor Dectin-1 in NAFLD. To our knowledge, we have provided the first empirical evidence of elevated levels of Dectin-1 in liver tissues from patients with NASH and in the HFD-induced mouse model of hepatic steatosis and fibrosis. Our main findings are summarized in the Graphic Abstract. We report that Dectin-1$^{-/-}$ mice fail to show the typical HFD-induced accumulation of lipids in hepatocytes and increased fibro-inflammatory responses. These protective effects of Dectin-1 deficiency were mediated by dampened Syk-NF-κB pathway. We further show that we can recapitulate these endpoints by administering HFD-fed mice with Dectin-1 inhibitor laminarin. Mechanistically, we show that macrophage Dectin-1 is necessary for palmitate-induced NF-κB activation and elaboration of cytokines such as TNFα, IL-6, and TGF-β1. These cytokines cause hepatocyte lipid accumulation, as found in cultured cells as well in the mouse model. Furthermore, these macrophage-derived factors cause hepatic stellate activation leading to increased fibro-genic responses. These effects are not seen when macrophage-derived factors are tested from Dectin-1 deficient macrophages. Together, these studies have discovered a new role of Dectin-1 in NAFLD and suggest that Dectin-1 may present a potential target to explore for the most common liver disease worldwide.

Components of innate immunity contribute to inflammatory NAFLD. HFD triggers a vigorous immune response, augmented by the generation and release of various inflammatory cytokines and chemokines, which ultimately exacerbate hepatic lipid accumulation and fibrosis. Activation of the immune response occurs mainly when damage-associated molecular patterns interact with

PRRs. PRRs contain four families Toll-like receptors, NOD-like receptors, C-type lectin receptors, and RIG-1-like receptors are expressed by the innate inflammatory cells. PRRs contains five major classes: Toll-like receptors (TLRs), NOD-like receptors (NLRs) and inflammasome, Retinoic acid-inducible gene-I-like receptors, C-type lectin receptors (CLRs), and Absent in melanoma 2-like receptors [41]. TLRs and NOD-like receptor P3 (NLRP3) inflammasome have been reported to be critically involved in inflammatory NAFLD [42]. However, to date, very little is known about the roles of CLRs in NAFLD. Our results demonstrated that Dectin-1 is highly expressed by hepatic macrophages in NAFLD. HFD was suggested to lead to an increase in the infiltration of Dectin-1$^+$ macrophages, which explained the elevated hepatic Dectin-1 expression in the liver. We demonstrate that Dectin-1, similar to TLRs and NLRP3, significantly contributes to the pathogenesis of NAFLD through mediating macrophage inflammation in liver.

Dectin-1 was first identified as a PRR of β-glucans in fungal pathogens [24]. To our best acknowledge, there is no other small-molecule ligands reported to be able to directly binds and activates Dectin-1. Recently, researchers studying alcoholic liver disease in mice fed an ethanol-containing diet observed increased levels of β-glucan to be associated with hepatic injury [43]. Treating these mice with anti-fungal agents reduced the severity of liver inflammation and injury. Importantly, they showed that Dectin-1 recognizes β-glucans and mediates alcohol-induced inflammatory liver injury [43]. These studies suggest that Dectin-1 may potentially mediate liver injury through hepatic fungal pathogens. In addition, Dectin-1 has been reported to ligate the lectin galectin-9 to promote pancreatic carcinoma immune-tolerance [44]. And, serum galectin-9 concentration has been reported to represent a potential biomarker of liver fibrosis in patients with chronic liver diseases [45]. Although our in vivo study could not exclude the possibility that Dectin-1 is activated by hepatic fungal pathogens or galectin-9 in NAFLD mice, our in vitro data (Fig. 5) showed that single PA incubation in cultured macrophages could quickly activate Dectin-1 as well as its downstream signals, indicating that, at least, Dectin-1 has endogenous ligands in PA-challenged macrophages. These results, plus with previous studies on Dectin-1 in sterile inflammatory diseases [19, 29], further point to non-pathogen-associated role of Dectin-1 in various pathologies.

Our results have led to an unanswered but important question. How does PA activate Dectin-1? Based on our current knowledge, the answer to this question may be related to TLR-crosstalk. There is evidence of a potential crosstalk between Dectin-1 and TLRs in hepatic injury. Dectin-1 has been shown to be upregulated in hepatic fibrosis and liver cancer [20]. However, when the researchers studied Dectin-1 deletion, it appeared to exacerbate liver fibro-inflammatory disease and accelerate hepatocarcinogenesis. In this model, Dectin-1 suppressed TLR4 signaling in hepatic inflammatory and stellate cells to provide protective effects [20]. In another model, Dectin-1 linked to TLR2 for an optimal production of TNF and IL-12 by dendritic cells exposed to zymosan [46]. Similarly, Brown and colleagues showed that a link between TLR2 and Dectin-1 signaling is necessary in macrophages for the production of TNF and IL-12 following zymosan treatment or infection with *C. albicans* conidia [47]. Finally, human peripheral blood mononuclear cells and monocyte-derived macrophages show synergy in TNF production when Dectin-1 is activated, together with TLR2 and TLR4 activation [48]. Precisely how Dectin-1 integrates with the TLRs is not known. Based on a few studies on TLR2, it is unlikely that there is actual physical interaction between TLRs and Dectin-1 [46]. One possibility is that Dectin-1 makes a higher order complex with TLRs through proximity, as has been established for lipopolysaccharide-MD2-CD14-TLR4 [49]. What these studies do suggest, however, is that it is highly possible that Dectin-1-mediated inflammatory responses seen in our in vivo and in vitro studies involved TLR activation. There is evidence that Dectin-1 requires MYD88 [50], adapter protein downstream of TLRs, and NF-κB [51] through TLRs. However, future studies are needed to dissect out these mechanisms in NAFLD.

Dectin-1 is specifically expressed in macrophages and other myeloid-monocytic lineage cells [9, 44]. Therefore, it is guessed that the phenotypes of systemic Dectin-1 knockout mice should be similar with that of macrophage-specific Dectin-1 knockout mice. In fact, all previously published papers about Dectin-1 and diseases used the whole-body Dectin-1 KO mice. This may be a common limitation of Dectin-1 studies. Anyway, using macrophage-specific Dectin-1 knockout in the study may be more accurate.

In conclusion, we have presented a comprehensive study that identified a novel role of Dectin-1 in NAFLD. Using a genetic knockout model and pharmacological interruption of Dectin-1 signaling, we showed that HFD-induced inflammatory responses in macrophages can be completely mitigated. Factors produced by macrophages with intact Dectin-1 cause hepatocytes to accumulate lipids and hepatic stellate cells to be activated and produce excessive fibrosis in the liver. Simply removing Dectin-1 gene or inhibiting the activity of this receptor in macrophages reduces the level of lipid accumulation in hepatocytes and associated fibro-inflammatory responses in the liver. Collectively, these studies clearly show an important role of Dectin-1 in NAFLD and suggest that Dectin-1 could potentially be targeted for therapy.

ACKNOWLEDGEMENTS

This study was supported by the National Key Research Project (2017YFA0506000 to GL), National Natural Science Foundation of China (81930108 to GL, 82000793 to WL, 81803600 to JCQ), and Zhejiang Provincial Key Scientific Project (2021C03041 to GL).

AUTHOR CONTRIBUTIONS

GL and WL contributed to the literature search and study design. GL, MXW, and WL participated in the drafting of the article. MXW, LY, LMJ, BY, and QHZ carried out the experiments. JCQ and YW revised the manuscript. YZ and WL contributed to data collection and analysis.

ADDITIONAL INFORMATION

Supplementary information The online version contains supplementary material available at https://doi.org/10.1038/s41401-022-00926-2.

Competing interests: The authors declare no competing interests.

REFERENCES

1. Kumar S, Duan Q, Wu R, Harris E, Su Q. Pathophysiological communication between hepatocytes and non-parenchymal cells in liver injury from NAFLD to liver fibrosis. Adv Drug Deliv Rev. 2021;176:113869.
2. Niu L, Sulek K, Vasilopoulou C, Santos A, Wewer Albrechtsen N, Rasmussen S, et al. Defining NASH from a Multi-Omics systems biology perspective. J Clin Med. 2021;10:4673.
3. Younossi ZM, Golabi P, de Avila L, Paik JM, Srishord M, Fukui N, et al. The global epidemiology of NAFLD and NASH in patients with type 2 diabetes: a systematic review and meta-analysis. J Hepatol. 2019;71:793–801.
4. Anstee QM, Reeves HL, Kotsiliti E, Govaere O, Heikenwalder M. From NASH to HCC: current concepts and future challenges. Nat Rev Gastroenterol Hepatol. 2019;16:411–28.
5. Ipsen DH, Lykkesfeldt J, Tveden-Nyborg P. Molecular mechanisms of hepatic lipid accumulation in non-alcoholic fatty liver disease. Cell Mol Life Sci. 2018;75:3313–27.
6. Todoric J, Di Caro G, Reibe S, Henstridge DC, Green CR, Vrbanac A, et al. Fructose stimulated de novo lipogenesis is promoted by inflammation. Nat Metab. 2020;2:1034–45.
7. Tacke F. Targeting hepatic macrophages to treat liver diseases. J Hepatol. 2017;66:1300–12.
8. Loomba R, Friedman SL, Shulman GI. Mechanisms and disease consequences of nonalcoholic fatty liver disease. Cell. 2021;184:2537–64.

9. Kalia N, Singh J, Kaur M. The role of dectin-1 in health and disease. Immunobiology. 2021;226:152071.
10. Mata-Martinez P, Bergon-Gutierrez M, Del Fresno C. Dectin-1 signaling update: new perspectives for trained immunity. Front Immunol. 2022;13:812148.
11. Strasser D, Neumann K, Bergmann H, Marakalala MJ, Guler R, Rojowska A, et al. Syk kinase-coupled C-type lectin receptors engage protein kinase C-delta to elicit Card9 adaptor-mediated innate immunity. Immunity. 2012;36:32–42.
12. Kingeter LM, Lin X. C-type lectin receptor-induced NF-kappaB activation in innate immune and inflammatory responses. Cell Mol Immunol. 2012;9:105–12.
13. Li X, Luo H, Ye Y, Chen X, Zou Y, Duan J, et al. betaglucan, a dectin1 ligand, promotes macrophage M1 polarization via NFkappaB/autophagy pathway. Int J Oncol. 2019;54:271–82.
14. Mentrup T, Stumpff-Niggemann AY, Leinung N, Schlosser C, Schubert K, Wehner R, et al. Phagosomal signalling of the C-type lectin receptor Dectin-1 is terminated by intramembrane proteolysis. Nat Commun. 2022;13:1880.
15. Campuzano A, Zhang H, Ostroff GR, Dos Santos Dias L, Wuthrich M, Klein BS, et al. CARD9-associated Dectin-1 and Dectin-2 are required for protective immunity of a multivalent vaccine against Coccidioides posadasii infection. J Immunol. 2020;204:3296–306.
16. Steele C, Marrero L, Swain S, Harmsen AG, Zheng M, Brown GD, et al. Alveolar macrophage-mediated killing of Pneumocystis carinii f. sp. muris involves molecular recognition by the Dectin-1 beta-glucan receptor. J Exp Med. 2003;198:1677–88.
17. Rahabi M, Jacquemin G, Prat M, Meunier E, AlaEddine M, Bertrand B, et al. Divergent roles for macrophage C-type lectin receptors, Dectin-1 and mannose receptors, in the intestinal inflammatory response. Cell Rep. 2020;30:4386–98 e5.
18. Chiba S, Ikushima H, Ueki H, Yanai H, Kimura Y, Hangai S, et al. Recognition of tumor cells by Dectin-1 orchestrates innate immune cells for anti-tumor responses. Elife. 2014;3:e04177.
19. Fan Q, Tao R, Zhang H, Xie H, Lu L, Wang T, et al. Dectin-1 contributes to myocardial ischemia/reperfusion injury by regulating macrophage polarization and neutrophil infiltration. Circulation. 2019;139:663–78.
20. Seifert L, Deutsch M, Alothman S, Alqunaibit D, Werba G, Pansari M, et al. Dectin-1 regulates hepatic fibrosis and hepatocarcinogenesis by suppressing TLR4 signaling pathways. Cell Rep. 2015;13:1909–21.
21. Smith AJ, Graves B, Child R, Rice PJ, Ma Z, Lowman DW, et al. Immunoregulatory activity of the natural product laminarin varies widely as a result of its physical properties. J Immunol. 2018;200:788–99.
22. Ding Z, Wang X, Liu S, Zhou S, Kore RA, Mu S, et al. NLRP3 inflammasome via IL-1beta regulates PCSK9 secretion. Theranostics. 2020;10:7100–10.
23. Marti-Rodrigo A, Alegre F, Moragrega AB, Garcia-Garcia F, Marti-Rodrigo P, Fernandez-Iglesias A, et al. Rilpivirine attenuates liver fibrosis through selective STAT1-mediated apoptosis in hepatic stellate cells. Gut. 2020;69:920–32.
24. Taylor PR, Tsoni SV, Willment JA, Dennehy KM, Rosas M, Findon H, et al. Dectin-1 is required for beta-glucan recognition and control of fungal infection. Nat Immunol. 2007;8:31–8.
25. Davison BA, Harrison SA, Cotter G, Alkhouri N, Sanyal A, Edwards C, et al. Suboptimal reliability of liver biopsy evaluation has implications for randomized clinical trials. J Hepatol. 2020;73:1322–32.
26. Peng C, Stewart AG, Woodman OL, Ritchie RH, Qin CX. Non-alcoholic steatohepatitis: a review of its mechanism, models and medical treatments. Front Pharmacol. 2020;11:603926.
27. Soret PA, Magusto J, Housset C, Gautheron J. In vitro and in vivo models of non-alcoholic fatty liver disease: a critical appraisal. J Clin Med. 2020;10:36.
28. Kleiner DE, Brunt EM, Van Natta M, Behling C, Contos MJ, Cummings OW, et al. Design and validation of a histological scoring system for nonalcoholic fatty liver disease. Hepatology. 2005;41:1313–21.
29. Ye XC, Hao Q, Ma WJ, Zhao QC, Wang WW, Yin HH, et al. Dectin-1/Syk signaling triggers neuroinflammation after ischemic stroke in mice. J Neuroinflammation. 2020;17:17.
30. Peng Y, Chen Y, Ma J, Zhou W, Wang Y, Wang Y, et al. Role and mechanism of the Dectin-1-mediated Syk/NF-kappaB signaling pathway in Talaromyces marneffei infection. Exp Ther Med. 2022;23:84.
31. Li X, Bian Y, Pang P, Yu S, Wang X, Gao Y, et al. Inhibition of Dectin-1 in mice ameliorates cardiac remodeling by suppressing NF-kappaB/NLRP3 signaling after myocardial infarction. Int Immunopharmacol. 2020;80:106116.
32. Li H, Xiao Y, Han L, Jia Y, Luo S, Zhang D, et al. Ganoderma lucidum polysaccharides ameliorated depression-like behaviors in the chronic social defeat stress depression model via modulation of Dectin-1 and the innate immune system. Brain Res Bull. 2021;171:16–24.
33. Goodridge HS, Reyes CN, Becker CA, Katsumoto TR, Ma J, Wolf AJ, et al. Activation of the innate immune receptor Dectin-1 upon formation of a 'phagocytic synapse'. Nature. 2011;472:471–5.
34. Luo X, Li H, Ma L, Zhou J, Guo X, Woo SL, et al. Expression of STING is increased in liver tissues from patients with NAFLD and promotes macrophage-mediated hepatic inflammation and fibrosis in mice. Gastroenterology. 2018;155:1971–84 e4.
35. Wang X, de Carvalho Ribeiro M, Iracheta-Vellve A, Lowe P, Ambade A, Satishchandran A, et al. Macrophage-specific hypoxia-inducible factor-1alpha contributes to impaired autophagic flux in nonalcoholic steatohepatitis. Hepatology. 2019;69:545–63.
36. Luo W, Ye L, Hu XT, Wang MH, Wang MX, Jin LM, et al. MD2 deficiency prevents high-fat diet-induced AMPK suppression and lipid accumulation through regulating TBK1 in non-alcoholic fatty liver disease. Clin Transl Med. 2022;12:e777.
37. Schwabe RF, Tabas I, Pajvani UB. Mechanisms of fibrosis development in nonalcoholic steatohepatitis. Gastroenterology. 2020;158:1913–28.
38. Yan J, Tung HC, Li S, Niu Y, Garbacz WG, Lu P, et al. Aryl hydrocarbon receptor signaling prevents activation of hepatic stellate cells and liver fibrogenesis in mice. Gastroenterology. 2019;157:793–806 e14.
39. Li J, Wang Y, Ma M, Jiang S, Zhang X, Zhang Y, et al. Autocrine CTHRC1 activates hepatic stellate cells and promotes liver fibrosis by activating TGF-beta signaling. EBioMedicine. 2019;40:43–55.
40. Dewidar B, Meyer C, Dooley S, Meindl-Beinker AN. TGF-beta in hepatic stellate cell activation and liver fibrogenesis-updated 2019. Cells. 2019;8:1419.
41. Wang X, Antony V, Wang Y, Wu G, Liang G. Pattern recognition receptor-mediated inflammation in diabetic vascular complications. Med Res Rev. 2020;40:2466–84.
42. Jin C, Flavell RA. Innate sensors of pathogen and stress: linking inflammation to obesity. J Allergy Clin Immunol. 2013;132:287–94.
43. Yang AM, Inamine T, Hochrath K, Chen P, Wang L, Llorente C, et al. Intestinal fungi contribute to development of alcoholic liver disease. J Clin Invest. 2017;127:2829–41.
44. Daley D, Mani VR, Mohan N, Akkad N, Ochi A, Heindel DW, et al. Dectin 1 activation on macrophages by galectin 9 promotes pancreatic carcinoma and peritumoral immune tolerance. Nat Med. 2017;23:556–67.
45. Fujita K, Niki T, Nomura T, Oura K, Tadokoro T, Sakamoto T, et al. Correlation between serum galectin-9 levels and liver fibrosis. J Gastroenterol Hepatol. 2018;33:492–9.
46. Gantner BN, Simmons RM, Canavera SJ, Akira S, Underhill DM. Collaborative induction of inflammatory responses by dectin-1 and Toll-like receptor 2. J Exp Med. 2003;197:1107–17.
47. Brown GD, Herre J, Williams DL, Willment JA, Marshall AS, Gordon S. Dectin-1 mediates the biological effects of beta-glucans. J Exp Med. 2003;197:1119–24.
48. Ferwerda G, Meyer-Wentrup F, Kullberg BJ, Netea MG, Adema GJ. Dectin-1 synergizes with TLR2 and TLR4 for cytokine production in human primary monocytes and macrophages. Cell Microbiol. 2008;10:2058–66.
49. Shimazu R, Akashi S, Ogata H, Nagai Y, Fukudome K, Miyake K, et al. MD-2, a molecule that confers lipopolysaccharide responsiveness on Toll-like receptor 4. J Exp Med. 1999;189:1777–82.
50. Kataoka K, Muta T, Yamazaki S, Takeshige K. Activation of macrophages by linear (1right-arrow3)-beta-D-glucans. Impliations for the recognition of fungi by innate immunity. J Biol Chem. 2002;277:36825–31.
51. Young SH, Ye J, Frazer DG, Shi X, Castranova V. Molecular mechanism of tumor necrosis factor-alpha production in 1->3-beta-glucan (zymosan)-activated macrophages. J Biol Chem. 2001;276:20781–7.